Received: 7 July 2017 | Accepted: 12 March 2018
DOI: 10.1002/jcp.26594

RAPID COMMUNICATION

WILEY Journal of Cellular Physiology

Early endplate remodeling and skeletal muscle signaling events following rat hindlimb suspension

Alexander V. Chibalin[1] | Boubacar Benziane[1] | Guzalija F. Zakyrjanova[2,3] | Violetta V. Kravtsova[2] | Igor I. Krivoi[2]

[1] Department of Molecular Medicine and Surgery, Integrative Physiology, Karolinska Institutet, Stockholm, Sweden

[2] Department of General Physiology, St. Petersburg State University, St. Petersburg, Russia

[3] Department of Normal Physiology, Kazan State Medical University, Kazan, Russia

Correspondence
Alexander V. Chibalin, Department of Molecular Medicine and Surgery, Integrative Physiology, Karolinska Institutet, Stockholm, Sweden.
Email: alexander.chibalin@ki.se
Igor I. Krivoi, Department of General Physiology, St. Petersburg State University, 7/9 University emb., St. Petersburg 199034, Russia.
Email: iikrivoi@gmail.com

Funding information
Swedish Research Council, Grant number: K2013-55X-14191-12-3; Novo Nordisk Foundation; Russian Foundation for Basic Research, Grant number: #16-04-00562; Strategic Research Program in Diabetes at Karolinska Institutet

Motor endplates naturally undergo continual morphological changes that are altered in response to changes in neuromuscular activity. This study examines the consequences of acute (6–12 hr) disuse following hindlimb suspension on rat soleus muscle endplate structural stability. We identify early changes in several key signaling events including markers of protein kinase activation, AMPK phosphorylation and autophagy markers which may play a role in endplate remodeling. Acute disuse does not change endplate fragmentation, however, it decreases both the individual fragments and the total endplate area. This decrease was accompanied by an increase in the mean fluorescence intensity from the nicotinic acetylcholine receptors which compensate the endplate area loss. Muscle disuse decreased phosphorylation of AMPK and its substrate ACC, and stimulated mTOR controlled protein synthesis pathway and stimulated autophagy. Our findings provide evidence that changes in endplate stability are accompanied by reduced AMPK phosphorylation and an increase in autophagy markers, and these changes are evident within hours of onset of skeletal muscle disuse.

KEYWORDS
AMPK, autophagy, endplate structure, hindlimb suspension, skeletal muscle

1 | INTRODUCTION

Skeletal muscle activity is crucial to maintain both muscle mass and muscle function. Mechanical unloading of skeletal muscle and reduced neuronal activity leads to dramatic remodeling events accompanied by loss of muscle mass, functional decline, and changes in the neuromuscular junction (Baldwin, Haddad, Pandorf, Roy, & Edgerton, 2013; Bodine, 2013; Wilson & Deschenes, 2005). Motor endplate represents specialized site on the post-synaptic plasma membrane by which the axon of a motor neuron establishes synaptic contact with a striated muscle fiber. Neuromuscular junction and endplate ultrastructure undergoes continual morphological remodeling which is amplified during conditions of altered neuromuscular activity. Increased activity, such as different modes of exercise training, typically results in expansion of the neuromuscular junction size. Reduced patterns of neuromuscular activity due to denervation, injury, bed rest, and other form of disuse including microgravity at spaceflight, various muscle diseases and aging, also triggers endplate remodeling (for review, see Gonzalez-Freire, de Cabo, Studenski, & Ferrucci, 2014; Nishimune, Stanford, & Mori, 2014; Rogers & Nishimune, 2017; Rudolf, Khan, Labeit, & Deschenes, 2014; Tintignac, Brenner, & Rüegg, 2015; Wilson & Deschenes, 2005). The molecular mechanisms underlying the effects of neuromuscular activity on endplate structure, function, and plasticity is complex and remains to be fully elucidated.

The later molecular events associated with overt skeletal muscle atrophy are well characterized. Much less is known about the early

molecular events which precede atrophy and operate within first days and even hours of disuse. These signaling events are of a special interest, highly debated and needs multiple time points of study to discover the molecular mechanisms that trigger disuse-induced functional alterations (Baehr et al., 2017; Baldwin et al., 2013; Vilchinskaya et al., 2017). Endplates specifically contribute to maintenance of the safety factor for neuromuscular transmission (Ruff, 2011; Wood & Slater, 2001) and endplate lipid raft disturbance is among the earliest remodeling events induced by skeletal muscle disuse (Petrov et al., 2017). Cholesterol and lipid rafts serve as a signaling platform for nicotinic acetylcholine receptors (nAChRs) clustering (Willmann et al., 2006; Zhu, Xiong, & Mei, 2006). Cholesterol is also important for Na,K-ATPase targeting and regulation (Cornelius, Habeck, Kanai, Toyoshima, & Karlish, 2015) and contribute to maintaining endplate electrogenesis (Kravtsova, Petrov, Vasiliev, Zefirov, & Krivoi, 2015). Moreover, it is established that the α2 Na,K-ATPase isozyme is enriched in endplate membrane where it co-localizes and functionally and molecularly interacts with the nAChRs (Chibalin et al., 2012; Heiny et al., 2010; Matchkov & Krivoi, 2016). The loss of α2 Na,K-ATPase activity accompanied by disturbances in lipid rafts are observed even after 6–12 hr of hindlimb suspension (Kravtsova et al., 2016; Petrov et al., 2017) suggesting the possibility of corresponding changes in the nAChRs distribution. Notably, in skeletal muscle, Na,K-ATPase activation depends on adenosine monophosphate-activated protein kinase (AMPK) (Benziane et al., 2012), a key regulator of glucose, lipid, and protein metabolism (Hardie, Schaffer, & Brunet, 2016). At the same time, skeletal muscle AMPK has been implicated in control of sarcolemma cholesterol levels (Ambery, Tackett, Penque, Brozinick, & Elmendorf, 2017; Habegger, Hoffman, Ridenour, Brozinick, & Elmendorf, 2012). In addition, AMPK and AMPK-activated autophagy have been implicated in neuromuscular junction remodeling (Carnio et al., 2014; Cerveró et al., 2016; Khan et al., 2014). Lowered contractile activity should provide an accumulation of phosphorylated high-energy phosphates and reduced AMPK activity, however, different studies demonstrated controversial data on the level of AMPK phosphorylation in rat soleus muscle after 1 day (Vilchinskaya et al., 2017) and after prolonged (Hilder et al., 2005) hindlimb suspension.

We propose that more precise time scale sampling within the first hours of disuse is necessary to provide a more complete picture of mechanisms underlying skeletal muscle atrophy. This time interval has not previously been adequately studied and 6–12 hr of hindlimb suspension were chosen for this study accordingly to α2 Na,K-ATPase and lipid rafts disturbances under these conditions (Kravtsova et al., 2016; Petrov et al., 2017). We hypothesized that early AMPK changes and AMPK-dependent signaling events are among key remodeling events accompanying the disuse-induced changes in the endplate stability. We analyzed the consequences of acute (6–12 hr) hindlimb suspension on the rat soleus muscle endplate structure determined from fluorescent labeling of the nAChRs with α-bungarotoxin, including quantification of individual neuromuscular junction fragmentation. We identify early changes in several key signaling events, including markers of protein kinase activation, AMPK phosphorylation and autophagy markers.

2 | MATERIALS AND METHODS

2.1 | Animal care and use

Experiments were performed on male Wistar rats (180–230 g). Animals were housed in a temperature- and humidity-controlled room with food and water ad libitum. All procedures involving rats were performed in accordance with the recommendations for the Guide for the Care and Use of Laboratory Animals (https://www.nap.edu/openbook.php?isbn_0309053773). The experimental protocol met the requirements of the EU Directive 2010/63/EU for animal experiments and was approved by the Bioethics Committee of Kazan State Medical University. The animals were subjected to hindlimb suspension individually in custom cages for 6 or 12 hr, as described previously (Morey-Holton, Globus, Kaplansky, & Durnova, 2005); control animals were not suspended. Soleus muscles were removed from euthanized animals. Freshly isolated muscles were used immediately for confocal microscopy imaging; some muscles were quickly frozen in liquid nitrogen for later biochemical assays.

2.2 | nAChRs staining and confocal microscopy imaging

To identify the endplate membrane region, tetramethylrhodamine-α-bungarotoxin (α-Btx, Biotium, Fremont, CA), a fluorescent-labeled specific ligand of the nAChRs was used. For imaging unfixed muscle, a freshly isolated soleus muscles with nerve stump were incubated for 15 min with physiological saline containing (mM) NaCl, 137; KCl, 5; $CaCl_2$, 2; $MgCl_2$, 2; $NaHCO_3$, 24; NaH_2PO_4, 1; glucose, 11; (pH 7.4) and 1 μM α-Btx followed by a 3 × 5 min wash. Saline was aerated with 95% O_2 and 5% CO_2 and maintained at room temperature. Superficial regions of the muscle were imaged with a ×63, 1.3 NA objective using a Leica TCS SP5 confocal system configured for viewing of rhodamine fluorescence. Analysis of endplate nAChRs fluorescence was performed in the region defined by α-Btx staining. Each distinct region of nAChRs labeling was outlined by hand. The degree of NMJs fragmentation, the area of each fragment and the fluorescence intensity from the nAChRs was determined from using ImageJ software.

2.3 | Analysis of signaling pathways

Frozen isolated soleus muscles were homogenized in lysis buffer (in mM: Tris-HCl 10, sucrose 250, EDTA 1, EGTA 1, Triton X–100 2%, pH 7.4; and one tablet protease inhibitor per 10 ml), the homogenate was centrifuged at 10,000*g* and the supernatant was collected. Protein concentration was determined using a bicinchoninic acid protein assay kit (Pierce, Rockford, IL). Protein lysates were subsequently diluted into Laemmle buffer and heated at 56 °C for 20 min.

To analyze signaling pathways, equal amounts of protein (15 μg) were separated on pre-cast Criterion SDS-PAGE gels of various percentages (Bio-Rad, Hercules, CA) and transferred to PVDF membranes (Immobilion, Millipore, MA). Equal loading of protein on gels was ensured using Ponceau staining. Membranes were blocked in

7.5% milk in TBS-T for 1 hr and incubated overnight with a primary antibody at +4 °C. Then, the membranes were washed and incubated with the appropriate horseradish peroxidase-conjugated secondary antibody (Bio-Rad) in 5% milk for 1 hr at room temperature. Proteins were visualized using enhanced chemiluminescence Western blotting detection reagents (GE Healthcare, Waukesha, WI). Optical density of the bands was quantified using Quantity One imaging system (Bio-Rad). Antibodies from Cell Signaling Technology (Beverly, MA) were: phospho-ACC Ser^{79}, phospho-AMPK Thr^{172}, phospho-mTOR Ser^{2448}, phospho-S6 ribosomal protein $Ser^{235/6}$, phospho-PKA substrate, which detects peptides and proteins containing a phospho-Ser/Thr residue with arginine at the -3 and -2 positions; pan-phosphoPKC Ser^{660} which detects PKC α, β I, β II, δ, ε, η, and θ isoforms; phosphorylated at a carboxy-terminal residue homologous to serine 660 of PKC β II; phospho Atg13 Ser^{355}; phospho-ULK1 Ser^{317}; phospho-ULK1 Ser^{757}; and LC3A/B, which recognizes total LC3A and LC3B proteins. Antibody p62/SQSTM1, which detects total SQSTM1/p62 protein, was from Sigma Aldrich (Saint Louis, MI). Antibody met PP2A Lys^{309} which detects Ser/Thr protein phosphatase 2A methylated at Lys^{309} was from Abcam (Cambridge, UK).

Detected protein was quantified using Quantity One software from Bio-Rad.

2.4 | Statistical analysis

Data are given as the mean ± SEM. Statistical significance of the difference between means was evaluated using a Student's *t*-test and one way ANOVA (ORIGIN Pro 8 software). Cumulative probability distributions were compared with the Kolmogorov-Smirnov test (GraphPad Prism 7 software). A probability value of $p < 0.05$ was taken to be statistically significant.

3 | RESULTS

3.1 | Acute hindlimb suspension induces early endplate structure remodeling

The control soleus muscle endplates were typically fragmented (Figure 1a) and the average number of fragments of nAChR-rich membrane at individual neuromuscular junctions were 3.0 ± 0.1 (382 fragments from 126 neuromuscular junctions, 17 muscles from 13 rats). After 6 and 12 hr of hindlimb suspension the average number of fragments were not significantly differ from control: respectively 2.8 ± 0.1 (409 fragments from 147 neuromuscular junctions, 18 muscles from 13 rats) and 3.4 ± 0.3 (191 fragments from 57 neuromuscular junction, 9 muscles from 5 rats) (Figures 1b and 1c). Corresponding cumulative probability curves were not significantly differing from control (Figure 1d) indicating stable level of fragmentation at short-term disuse.

After 6 and 12 hr of hindlimb suspension, distribution of fragments area and corresponding cumulative probability curves were significantly ($p < 0.05$ and $p < 0.01$, respectively) shifted toward fewer values compared to control (Figure 1e) suggesting the decrease of individual fragments area. The fragments area distribution in the control was best fitted by a Gaussian three-peak model indicating the dominance of relatively large fragments with average area 145 ± 10 μm^2 (Figure 1f). Similar distributions were obtained after 6 and 12 hr of hindlimb suspension, however the average area of large fragments and their contribution to overall distributions were decreased (Figures 1g and 1h) accordingly to left shift of corresponding cumulative curves (Figure 1e).

The total area of each individual endplate was determined as the sum of its fragments area. The average endplate area in control soleus muscles was 375 ± 14 μm^2 and decreased by 27% ($p < 0.01$) and 40% ($p < 0.01$) after 6 and 12 hr of hindlimb suspension, respectively (Figure 1i). This decrease accompanied by increase in the mean fluorescence intensity from the nAChRs by 10% and 37% ($p < 0.01$), respectively (Figure 1j). As result, the average total nAChRs fluorescence from the individual endplates was decreased only after 6 hr of hindlimb suspension and was not differ from control after 12 hr of hindlimb suspension (Figure 1k).

3.2 | Acute hindlimb suspension induces early changes in stress, metabolic, and autophagy pathways

Changes in the activity of protein kinases and phosphatases mediate many downstream signaling pathways. Acute (6–12 hr) hindlimb suspension changed the activity of PKC and PKA, evident as a transient increase in auto-phosphorylation of PKCs and phosphorylation of PKA substrates (anti phospho PKA substrate). Accordingly the abundance of the active methylated form of protein phosphatase 2A decreased. In contrast, acute hindlimb suspension decreased the phosphorylation of AMPK and its substrate ACC (Figures 2a and e), that may tend to decrease in fatty acid oxidation and rerouting fatty acid toward triglyceride synthesis and storage in unused muscles. These results suggest that acute hindlimb suspension alters character of kinases activation and downregulates pathways involved in fatty acid metabolism.

The abundance of skeletal muscle proteins is tightly controlled by anabolic and catabolic signaling. In rat skeletal muscle, stimulation of protein synthesis is associated with activation of protein kinases in the mammalian target of rapamycin (mTOR) signal transduction pathway (Bolster, Crozier, Kimball, & Jefferson, 2002). Six hours of hindlimb suspension increased the phosphorylation of mTOR (Ser^{2448}) and ribosomal protein S6 ($Ser^{235/6}$), and both returned toward control levels after 12 hr of hindlimb suspension (Figures 2b and e). The early transient increase in phospho-mTOR indicates that 6 hr of hindlimb suspension could maintain protein synthesis via the mTOR-p70S6 kinase pathway.

We also examined pERK1/2 MAP kinase, a stress activated kinase that signal toward protein synthesis and found that the phosphorylation of ERK1/2 MAP kinase transiently increases after 6 hr of hindlimb suspension (Figures 2b and e). Notably, the phosphorylation of the mechanical- and osmotic-stress responsive kinase p38 was unaltered (data not shown). The protein abundance of SERCA1,

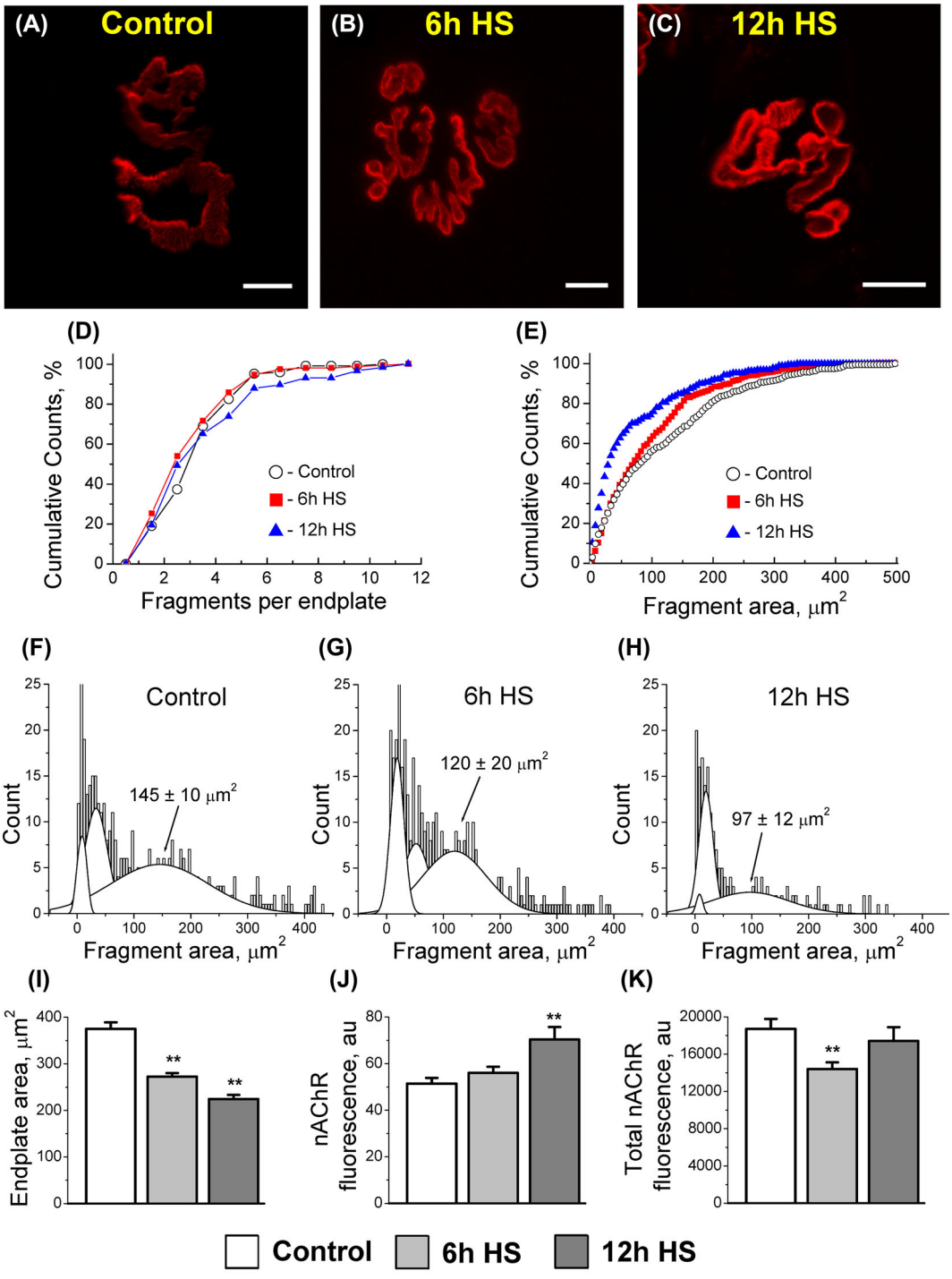

FIGURE 1 Soleus muscle endplates remodeling after short-term hindlimb suspension. Representative images of nAChR distribution. (a) A rat soleus muscle was labeled with rhodamine-conjugated α-bungarotoxin (red channel) to visualize nAChR localization. (b and c) Same labeling after 6 and 12 hr of hindlimb suspension, respectively. Calibration bars—10 μm. (d and e) Cumulative histograms of the number of fragments present at the endplates and of the fragments area in control and after 6 or 12 hr of hindlimb suspension. (f, g and h) The fragments area distribution in control and after 6 or 12 hr of hindlimb suspension. (i, j and k) The total stained nAChR area, the fluorescence intensity (arbitrary units) from the nAChRs and total nAChRs fluorescence from the individual endplates in control and after 6 or 12 hr of hindlimb suspension. Bars represent mean ± SEM. $^{**}p < 0.01$ compared to corresponding control. Control—126 NMJs, 17 muscles from 13 rats; 6 hr of hindlimb suspension—147 NMJs, 18 muscles from 13 rats; 12 hr of hindlimb suspension—57 NMJs, 9 muscles from 5 rats

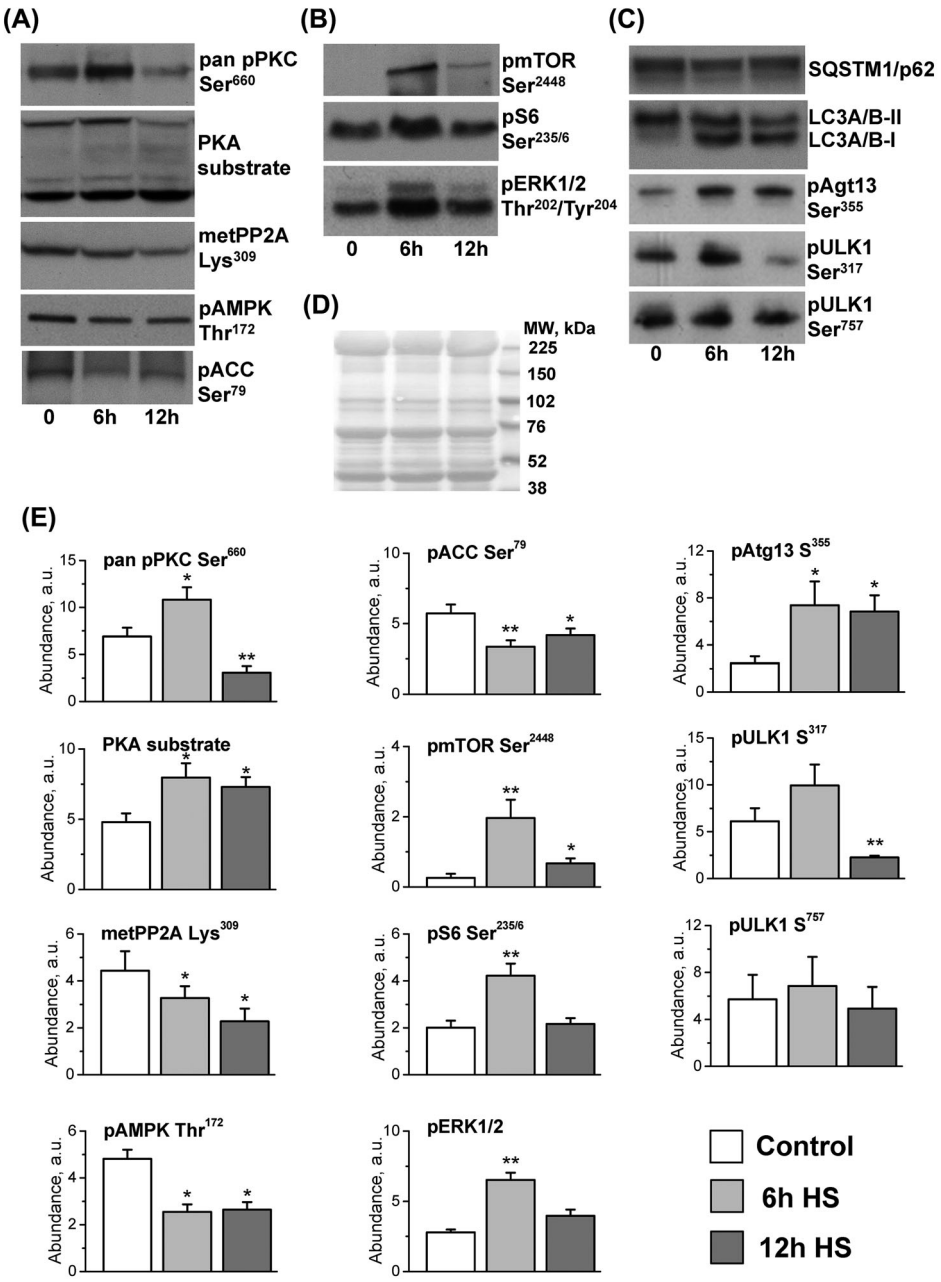

FIGURE 2 Molecular signaling events in rat soleus muscle after 6 and 12 hr of hindlimb suspension. (a and b) Protein kinase activation/phosphorylation and protein synthesis markers. (c) Autophagy markers. (d) Ponceau S staining to verify equal loading. Blots are representative of measurements for 6–10 independent muscle samples. (e) Quantification of signaling markers abundance changes. Relative bar graphs of the mean density of measurements for 8–10 independent muscle samples are shown. Y-axis, arbitrary units. $^{*}p < 0.05$; $^{**}p < 0.01$ compared to corresponding control

SERCA2, and phospholamban was unchanged by hindlimb suspension (data not shown). Therefore, acute hindlimb suspension stimulates stress signaling pathways that promote protein synthesis.

In autophagic processes, the adapter protein SQSTM1/p62 (sequestosome 1) interacts with autophagosomal membrane protein LC3A/B-II to promote entry of ubiquitinated cargo into the autophagosome (Sakuma, Aoi, & Yamaguchi, 2014). After 6 hr of hindlimb suspension, the decrease in abundance of SQSTM1/p62 and increase in LC3A/B-II (Figure 2c), indicate an increase in autophagy in the muscle. Mammalian Atg13 forms a complex with the ULK1/2, which localizes to autophagic isolation membranes and regulates autophagosome biogenesis. ULK1-dependent phosphorylation of Atg13 at Ser^{355}, leads to the recruitment of Atg13 to damaged mitochondria, enabling efficient mitophagy (Martin-Rincon, Morales-Alamo, & Calbet, 2017). AMPK, activated during low nutrient conditions, directly phosphorylates ULK1 at multiple sites (Ha, Guan, & Kim, 2015). Conversely, mTOR, which is an inhibitor of autophagy, phosphorylates ULK1 at Ser^{757} and disrupts the interaction

between ULK1 and AMPK (Martin-Rincon et al., 2017). However, despite the increased mTOR phosphorylation at Ser^{2448} (Figures 2b and 2e) we do not see an increase in ULK1 phosphorylation at Ser^{757} (Figures 2c and e). At the same time phosphorylation of both Atg13 at Ser^{355} and ULK1 at Ser^{317} elevated (Figures 2c and 2e), suggesting an increase in autophagy.

4 | DISCUSSION

Prolonged mechanical unloading of skeletal muscle as well as reduced neuromuscular activity leads to muscle wasting and functional decline (Baehr et al., 2017; Baldwin et al., 2013; Bodine, 2013) including the loss of neuromuscular junction integrity (Gonzalez-Freire et al., 2014; Nishimune et al., 2014; Rudolf et al., 2014; Tintignac et al., 2015; Wilson & Deschenes, 2005). A more complete understanding of the early disuse-induced molecular events is needed to identify important signaling pathways that lead to endplate disturbance. Our study provides the first evidence that endplate remodeling is accompanied by changes in protein kinase activation, and AMPK phosphorylation and autophagy markers, are among the earliest events observed within hours of onset of skeletal muscle disuse.

The precise mechanisms of the observed endplate area decrease and simultaneous increase in the fluorescence intensity from the nAChRs are currently not known. This increase can reflect the enhanced density of the nAChRs distribution as an adaptive response to the endplate area loss. Autophagy is known to regulate basal and atrophy-induced turnover of the nAChRs (Khan et al., 2014). Thus, an increased density of the nAChRs distribution after acute hindlimb suspension can result from increased autophagy (this study) rather than from other mechanisms. Cholesterol is essential for nAChR function and direct molecular nAChR-cholesterol interactions are proposed (Brannigan, Hénin, Law, Eckenhoff, & Klein, 2008). Cholesterol and lipid microdomains serve as signaling platforms for the nAChRs and stabilize the endplate at the neuromuscular junction (Willmann et al., 2006; Zhu et al., 2006). Therefore the lipid rafts disturbance, observed after 6–12 hr of hindlimb suspension (Petrov et al., 2017) can be involved in early endplate remodeling.

AMPK is an energy-sensing enzyme (Hardie et al., 2016) that is known to be a critical regulator of metabolism, transcription, and muscle phenotype. Early hindlimb suspension-induced endplate remodeling was accompanied by a two-fold decrease in AMPK and ACC phosphorylation (Figure 2e). A significant decrease in phospho-AMPK content was observed in rat soleus muscle after 24 hr of hindlimb suspension (Mirzoev, Tyganov, Vilchinskaya, Lomonosova, & Shenkman, 2016) and after 3 days of the dry immersion (on-ground simulation model of gravitational unloading) in human soleus muscle (Vilchinskaya, Mirzoev, Lomonosova, Kozlovskaya, & Shenkman, 2015). Decreased phosphorylation of AMPK and ACC may be associated with the impaired balance of phosphorylated and dephosphorylated high-energy purine nucleotides (ATP/ADP/AMP) during hindlimb suspension. Decreased ATP usage for contraction, and ion transport by SERCA and Na,K-ATPase, could translate into increased ATP/AMP ratio, thus inactivating AMPK, activating ACC and decreasing the absolute level of fatty acid oxidation.

Pharmacological activation of AMPK prevents skeletal muscle atrophy and structural changes in neuromuscular junctions in a mouse model of spinal muscular atrophy (Cerveró et al., 2016), ameliorates muscular dystrophy in the mdx mouse (Ljubicic & Jasmin, 2013) and prevents early atrophic signaling events in the rat soleus muscle after 24 hr of hindlimb suspension (Vilchinskaya et al., 2017). Notably, AMPK may play a role in activating PGC-1α which has been suggested as a key protein involved in maintaining neuromuscular junction integrity (Gonzalez-Freire et al., 2014; Nishimune, Stanford, & Mori, 2014). PGC-1α over-expression suppresses mouse soleus muscles atrophy during prolonged (3–14 days) hindlimb suspension (Wang et al., 2017). Additionally, AMPK plays a role in adaptive changes, including autophagy. Autophagy is involved in nAChRs turnover (Khan et al., 2014) and impairments in autophagy induce neuromuscular junction degeneration (Carnio et al., 2014). Accordingly, an increase in autophagy after hindlimb suspension (Figure 2e) can reflect normal adaptive response to stabilize the endplate configuration. Notably, Atg13 and ULK1 phosphorylation does not correlate with increase in AMPK activation (this study). The discrepancy could be explained by involvement of different pools of AMPK, signaling toward metabolic and autophagic pathways (Pinter, Grignani, Watkins, & Redwood, 2013).

In summary, neuromuscular junction rapidly (within hours) responds to skeletal muscle disuse as manifested by the loss of α2 Na,K-ATPase activity (Kravtsova et al., 2016) accompanied by disturbance of lipid rafts (Petrov et al., 2017) and changes in endplate stability (this study). Little is known about very complex initial steps of skeletal muscle atrophy involving number cross-talked signaling pathways. Our findings provide evidence to suggest that changes in AMPK phosphorylation and autophagy markers are among earlier key disuse-induced remodeling events. Also, our data confirm that lowered contractile activity is initially accompanied by reduced AMPK activity in contrast with prolonged disuse which has an opposite effect (Hilder et al., 2005). Further data sampling at multiple time points is required to complete our knowledge and provide insight into early molecular mechanisms following disuse. Moreover, determining the key early signaling response to disuse provides the possibility for precise and effective interventions for preventing atrophy. This knowledge should reveal a possible drug target which could maintain skeletal muscle function to prevent an overt atrophy in humans.

ACKNOWLEDGMENTS

This work was supported by Russian Foundation for Basic Research #16-04-00562; by Swedish Research Council #K2013-55X-14191-12-3, Novo Nordisk Foundation and Strategic Research Program in Diabetes at Karolinska Institutet. We thank Dr. Anna Krook for the critical reading the manuscript. We are very grateful to St. Petersburg State University research Center for Molecular and Cell Technologies and personally to Nikolai A. Kostin for assistance with confocal microscopy experiments.

AUTHORS' CONTRIBUTION

AVC and IIK conception and design of research; AVC, BB, GFZ, and VVK performed experiments; AVC, BB, GFZ, and VVK, analyzed data; AVC, VVK, and IIK interpreted results of experiments; AVC, VVK, and IIK prepared figures; AVC and IIK drafted and edited manuscript; AVC, BB, GFZ, VVK, and IIK approved final version of manuscript.

CONFLICTS OF INTEREST

The authors declare no competing financial interests.

ORCID

Alexander V. Chibalin http://orcid.org/0000-0002-6339-6271

REFERENCES

Ambery, A. G., Tackett, L., Penque, B. A., Brozinick, J. T., & Elmendorf, J. S. (2017). Exercise training prevents skeletal muscle plasma membrane cholesterol accumulation, cortical actin filament loss, and insulin resistance in C57BL/6J mice fed a western-style high-fat diet. *Physiological Reports*, *5*(16), e13363.

Baehr, L. M., West, D. W. D., Marshall, A. G., Marcotte, G. R., Baar, K., & Bodine, S. C. (2017). Muscle-specific and age-related changes in protein synthesis and protein degradation in response to hindlimb unloading in rats. *Journal of Applied Physiology* (1985), *122*(5), 1336–1350.

Baldwin, K. M., Haddad, F., Pandorf, C. E., Roy, R. R., & Edgerton, V. R. (2013). Alterations in muscle mass and contractile phenotype in response to unloading models: Role of transcriptional/pretranslational mechanisms. *Frontiers in Physiology*, *4*, 284.

Benziane, B., Bjornholm, M., Pirkmajer, S., Austin, R. L., Kotova, O., Viollet, B., . . . Chibalin, A. V. (2012). Activation of AMP-activated protein kinase stimulates Na^+,K^+-ATPase activity in skeletal muscle cells. *The Journal of Biological Chemistry*, *287*, 23451–23463.

Bodine, S. C. (2013). Disuse-induced muscle wasting. *International Journal of Biochemistry & Cell Biology*, *45*, 2200–2208.

Bolster, D. R., Crozier, S. J., Kimball, S. R., & Jefferson, L. S. (2002). AMP-activated protein kinase suppresses protein synthesis in rat skeletal muscle through down-regulated mammalian target of rapamycin (mTOR) signaling. *The Journal of Biological Chemistry*, *277*, 23977–23980.

Brannigan, G., Hénin, J., Law, R., Eckenhoff, R., & Klein, M. L. (2008). Embedded cholesterol in the nicotinic acetylcholine receptor. *Proceedings of the National Academy of Sciences of the United States of America*, *105*, 14418–14423.

Carnio, S., LoVerso, F., Baraibar, M. A., Longa, E., Khan, M. M., Maffei, M., . . . Sandri, M. (2014). Autophagy impairment in muscle induces neuromuscular junction degeneration and precocious aging. *Cell Reports*, *8*, 1509–1521.

Cerveró, C., Montull, N., Tarabal, O., Piedrafita, L., Esquerda, J. E., & Calderó, J. (2016). Chronic treatment with the AMPK agonist AICAR prevents skeletal muscle pathology but fails to improve clinical outcome in a mouse model of severe spinal muscular atrophy. *Neurotherapeutics*, *13*, 198–216.

Chibalin, A. V., Heiny, J. A., Benziane, B., Prokofiev, A. V., Vasiliev, A. N., Kravtsova, V. V., & Krivoi, I. I. (2012). Chronic nicotine exposure modifies skeletal muscle Na, K-ATPase activity through its interaction with the nicotinic acetylcholine receptor and phospholemman. *PLoS ONE*, *7*, e33719.

Cornelius, F., Habeck, M., Kanai, R., Toyoshima, C., & Karlish, S. J. (2015). General and specific lipid-protein interactions in Na,K-ATPase. *Biochimica Et Biophysica Acta*, *1848*, 1729–1743.

Gonzalez-Freire, M., de Cabo, R., Studenski, S. A., & Ferrucci, L. (2014). The neuromuscular junction: Aging at the crossroad between nerves and muscle. *Frontiers in Aging Neuroscience*, *6*, 208.

Ha, J., Guan, K. L., & Kim, J. (2015). AMPK and autophagy in glucose/glycogen metabolism. *Molecular Aspects of Medicine*, *46*, 46–62.

Habegger, K. M., Hoffman, N. J., Ridenour, C. M., Brozinick, J. T., & Elmendorf, J. S. (2012). AMPK enhances insulin-stimulated GLUT4 regulation via lowering membrane cholesterol. *Endocrinology*, *153*, 2130–2141.

Hardie, D. G., Schaffer, B. E., & Brunet, A. (2016). AMPK: An energy-sensing pathway with multiple inputs and outputs. *Trends in Cell Biology*, *26*, 190–201.

Heiny, J. A., Kravtsova, V. V., Mandel, F., Radzyukevich, T. L., Benziane, B., Prokofiev, A. V., . . . Krivoi, I. I. (2010). The nicotinic acetylcholine receptor and the Na,K-ATPase α2 isoform interact to regulate membrane electrogenesis in skeletal muscle. *The Journal of Biological Chemistry*, *285*, 28614–28626.

Hilder, T. L., Baer, L. A., Fuller, P. M., Fuller, C. A., Grindeland, R. E., Wade, C. E., & Graves, L. M. (2005). Insulin-independent pathways mediating glucose uptake in hindlimb-suspended skeletal muscle. *Journal of Applied Physiology* (1985), *99*, 2181–2188.

Khan, M. M., Strack, S., Wild, F., Hanashima, A., Gasch, A., Brohm, K., . . . Rudolf, R. (2014). Role of autophagy, SQSTM1, SH3GLB1, and TRIM63 in the turnover of nicotinic acetylcholine receptors. *Autophagy*, *10*, 123–136.

Kravtsova, V. V., Petrov, A. M., Matchkov, V. V., Bouzinova, E. V., Vasiliev, A. N., Benziane, B., . . . Krivoi, I. I. (2016). Distinct α2 Na,K-ATPase membrane pools are differently involved in early skeletal muscle remodeling during disuse. *Journal of General Physiology*, *147*, 175–188.

Kravtsova, V. V., Petrov, A. M., Vasiliev, A. N., Zefirov, A. L., & Krivoi, I. I. (2015). Role of cholesterol in the maintenance of endplate electrogenesis in rat diaphragm. *Bulletin of Experimental Biology and Medicine*, *158*, 298–300.

Ljubicic, V., & Jasmin, B. J. (2013). AMP-activated protein kinase at the nexus of therapeutic skeletal muscle plasticity in Duchenne muscular dystrophy. *Trends in Molecular Medicine*, *19*, 614–624.

Martin-Rincon, M., Morales-Alamo, D., & Calbet, J. A. L. (2018). Exercise-mediated modulation of autophagy in skeletal muscle. *Scandinavian Journal of Medicine and Science in Sports*, *28*, 772–781.

Matchkov, V. V., & Krivoi, I. I. (2016). Specialized functional diversity and interactions of the Na, K-ATPase. *Frontiers in Physiology*, *7*, 179.

Mirzoev, T., Tyganov, S., Vilchinskaya, N., Lomonosova, Y., & Shenkman, B. (2016). Key markers of mTORC1-dependent and mTORC1-independent signaling pathways regulating protein synthesis in rat soleus muscle during early stages of hindlimb unloading. *Cellular Physiology and Biochemistry*, *39*, 1011–1020.

Morey-Holton, E., Globus, R. K., Kaplansky, A., & Durnova, G. (2005). The hindlimb unloading rat model: Literature overview, technique update and comparison with space flight data. *Advances in Space Biology and Medicine*, *10*, 7–40.

Nishimune, H., Stanford, J. A., & Mori, Y. (2014). Role of exercise in maintaining the integrity of the neuromuscular junction. *Muscle and Nerve*, *49*, 315–324.

Petrov, A. M., Kravtsova, V. V., Matchkov, V. V., Vasiliev, A. N., Zefirov, A. L., Chibalin, A. V., . . . Krivoi, I. I. (2017). Membrane lipid rafts are disturbed in the response of rat skeletal muscle to short-term disuse. *American Journal of Physiology Cell Physiology*, *312*, C627–C637.

Pinter, K., Grignani, R. T., Watkins, H., & Redwood, C. (2013). Localisation of AMPK g subunits in cardiac and skeletal muscles. *Journal of Muscle Research and Cell Motility*, *34*, 369–378.

Rogers, R. S., & Nishimune, H. (2017). The role of laminins in the organization and function of neuromuscular junctions. *Matrix Biology*, *57-58*, 86–105.

Rudolf, R., Khan, M. M., Labeit, S., & Deschenes, M. R. (2014). Degeneration of neuromuscular junction in age and dystrophy. *Frontiers in Aging Neuroscience*, *6*, 99.

Ruff, R. L. (2011). Endplate contributions to the safety factor for neuromuscular transmission. *Muscle and Nerve*, *44*, 854–861.

Sakuma, K., Aoi, W., & Yamaguchi, A. (2014). The intriguing regulators of muscle mass in sarcopenia and muscular dystrophy. *Frontiers in Aging Neuroscience*, *6*, 230.

Tintignac, L. A., Brenner, H. R., & Rüegg, M. A. (2015). Mechanisms regulating neuromuscular junction development and function and causes of muscle wasting. *Physiological Reviews*, *95*, 809–852.

Vilchinskaya, N. A., Mirzoev, T. M., Lomonosova, Y. N., Kozlovskaya, I. B., & Shenkman, B. S. (2015). Human muscle signaling responses to 3-day head-out dry immersion. *Journal of Musculoskeletal and Neuronal Interactions*, *15*, 286–293.

Vilchinskaya, N. A., Mochalova, E. P., Nemirovskaya, T. L., Mirzoev, T. M., Turtikova, O. V., & Shenkman, B. S. (2017). Rapid decline in MyHC I(β) mRNA expression in rat soleus during hindlimb unloading is associated with AMPK dephosphorylation. *Journal of Physiology*, *595*, 7123–7134.

Wang, J., Wang, F., Zhang, P., Liu, H., He, J., Zhang, C., . . . Chen, X. (2017). PGC-1α over-expression suppresses the skeletal muscle atrophy and myofiber-type composition during hindlimb unloading. *Bioscience, Biotechnology, and Biochemistry*, *81*, 500–513.

Willmann, R., Pun, S., Stallmach, L., Sadasivam, G., Santos, A. F., Caroni, P., & Fuhrer, C. (2006). Cholesterol and lipid microdomains stabilize the postsynapse at the neuromuscular junction. *EMBO Journal*, *25*, 4050–4060.

Wilson, M. H., & Deschenes, M. R. (2005). The neuromuscular junction: Anatomical features and adaptations to various forms of increased, or decreased neuromuscular activity. *International Journal of Neuroscience*, *115*, 803–828.

Wood, S. J., & Slater, C. R. (2001). Safety factor at the neuromuscular junction. *Progress in Neurobiology*, *64*, 393–429.

Zhu, D., Xiong, W. C., & Mei, L. (2006). Lipid rafts serve as a signaling platform for nicotinic acetylcholine receptor clustering. *The Journal of Neuroscience: The Official Journal of the Society for Neuroscience*, *26*, 4841–4851.

How to cite this article: Chibalin AV, Benziane B, Zakyrjanova GF, Kravtsova VV, Krivoi II. Early endplate remodeling and skeletal muscle signaling events following rat hindlimb suspension. *J Cell Physiol*. 2018;233:6329–6336. https://doi.org/10.1002/jcp.26594